





Quantum-inspired entanglement between collaborating brains during human memory encoding

Xue Yang^a, Yi Jiang^{b,c} , Qianxiang Zhou^{d,e}, Kuan Pei^f, Chunyan Guo^{a,1}, and Peng Zhang^{a,1} 

Affiliations are included on p. 11.

Edited by Terrence Sejnowski, Salk Institute for Biological Studies, La Jolla, CA; received July 31, 2025; accepted February 9, 2026

The extent to which two brains align during information processing is thought to be central to collaborative memory encoding; however, the neural mechanisms that support such interpersonal alignment remain elusive. Traditional interbrain synchrony models based on phase-alignment metrics fail to distinguish true interbrain connectivity from spurious synchrony driven by shared stimulus processing. Here, we introduce a quantum-inspired framework to capture the connectivity between two collaborating brains. Using dual-brain Electroencephalogram (EEG) hyperscanning, we quantified interbrain coupling during collaborative (Colla)-memory and independent (Indep)-memory encoding in two experiments, including 70 dyads ($N = 140$) in Experiment 1 and 41 dyads ($N = 82$) in Experiment 2, which incorporated an empathy-enhancement training procedure. Treating Indep as a baseline state, we found that Colla without training deviated from this baseline by showing a higher probability of $|aligned\rangle$ states and a lower probability of $|misaligned\rangle$ states. Following empathy enhancement, Colla state probabilities returned toward the Indep baseline, accompanied by parallel normalization in memory retrieval performance and a shift in the cortical distribution of Colla-Indep differences toward regions implicated in socioemotional processing. Together, the Quantum Aligned-Misaligned Entanglement Model demonstrates that interbrain connectivity dynamics during memory encoding are context sensitive, dynamically evolving with cooperative engagement, and can be reshaped by empathic interaction in ways that systematically relate to subsequent retrieval performance. These findings suggest that quantum-inspired entanglement can be applied to modeling interbrain neural connectivity, offering a framework for understanding collaborative memory encoding.

Quantum entanglement | Interbrain connectivity | Collaborative memory encoding | $|aligned\rangle$ | $|misaligned\rangle$

Memory encoding across collaborating brains is fundamental to everyday social behavior. For example, when two young musicians rehearse a concerto, they must encode shared musical structure while synchronizing tempo and timing (1, 2). Compared with independent encoding, collaborative-memory encoding imposes greater cognitive demands, requiring neural mechanisms that support information sharing and coordinated processing across brains, and engaging additional spatial and temporal neural patterns (3–5). Despite its importance, the neural basis of collaborative-memory encoding remains poorly understood. A central challenge lies in characterizing connectivity between interacting brains, which is not mediated by any tangible physical medium (6–8) and has therefore been likened to quantum entanglement, where nonlocal correlations emerge between spatially separated particles (9).

Neural synchrony metrics, including phase-locking value (PLV), weighted phase lag index (WPLI), and phase-amplitude coupling, are widely used to quantify functional connectivity within a single brain (10–13). However, these measures can be misleading when applied to interactions between two brains, as synchrony may arise even during independent task performance across different times or locations (14, 15). As noted by Holroyd, two neural time series can exhibit stable phase or amplitude relationships simply by sharing a common oscillatory frequency, independent of true interbrain coupling (16). Consequently, external stimuli can induce apparent synchrony across uncooperative brains, such as when individuals memorize the same musical material separately (7, 17, 18). Although synchrony indices remain useful for characterizing temporal alignment across brains (19–21), including high-gamma coordination between the temporoparietal junction and amygdala (22, 23), they do not, by themselves, distinguish genuine interpersonal connectivity from stimulus-driven synchrony.

Here we seek indices that characterize genuine connectivity between two cooperating brains, rather than relying solely on measures of neural synchrony, in a context where

Significance

This study introduces a neurophysiological quantum-inspired cognition framework grounded in dual-brain Electroencephalogram (EEG) data. We develop and validate the Quantum Aligned-Misaligned Entanglement Model (QAEM), which distinguishes collaborative-memory from independent-memory encoding by identifying socially driven interbrain coupling, overcoming limitations of traditional synchrony metrics that confound interpersonal coupling with stimulus-driven synchrony. Our results show that collaborative encoding selectively modulates familiarity-based memory retrieval, and that this effect is systematically associated with context-dependent changes in interbrain entanglement. Moreover, empathic context reshapes the relationship between neural coupling and memory performance, indicating that interbrain coordination reflects flexible interpersonal dynamics rather than fixed individual traits. Together, these findings provide a principled neural framework for understanding how social interaction shapes memory through dynamic interbrain coordination.

This article is a PNAS Direct Submission.

Copyright © 2026 the Author(s). Published by PNAS. This article is distributed under Creative Commons Attribution-NonCommercial-NoDerivatives License 4.0 (CC BY-NC-ND).

¹To whom correspondence may be addressed. Email: guocy@cnu.edu.cn or b494@cnu.edu.cn.

This article contains supporting information online at <https://www.pnas.org/lookup/suppl/doi:10.1073/pnas.2520834123/-/DCSupplemental>.

Published March 11, 2026.

neural activities interact without an observable signal transmission medium (24, 25). This interaction pattern invites comparison with quantum entanglement, in which nonlocal correlations arise between spatially separated particles whose states cannot be described independently (26, 27). Notably, Bohr proposed that quantum principles might extend beyond physics to broader domains of human knowledge (28, 29), motivating the application of quantum formalism in cognitive modeling (30–32). Previous studies have shown that quantum probability theory accounts for cognitive phenomena that violate classical assumptions, including the disjunction effect in decision-making (33–35), quantum interference in perceptual judgments (36), quantum random walk advantages in perceptual decision tasks (37), and quantum-like internal state representations in the medial frontal cortex during value-based learning (38).

In human memory research, quantum mathematical models incorporating superposition and entanglement have been used to explain phenomena that violate classical probability theory (28, 39, 40). For example, quantum models of recognition memory formalize retrieval as a superposition of potential states that collapses upon cue presentation, providing a probabilistic account of fuzzy trace theory (41). Similarly, entanglement-based memory models have been applied to semantic priming, in which parallel activation across semantic associates produces context-dependent memory facilitation (42). Building on these advances, we propose that collaborative-memory encoding between two individuals may be more effectively described using a quantum-inspired formalism, particularly entanglement representations, manifesting as aligned or misaligned interbrain states (e.g., |aligned>, |misaligned>) in which shared information processing and memory encoding are dynamically interdependent.

Although prior studies have proposed quantum-inspired frameworks for modeling cognitive phenomena or drawn analogies between entanglement and human behavior, these approaches have largely relied on behavioral simulations (39), speculative assumptions about consciousness linkage, or experimental paradigms involving special populations such as monozygotic twins (43). In contrast, we introduce a neurophysiological modeling framework that constructs effective entanglement representations directly from dual-brain EEG recorded during real-time cooperation. Rather than inferring entanglement from behavioral anomalies or conceptual analogies (29, 39), we operationalize it empirically by mapping interbrain synchrony measures onto a quantum-inspired two-qubit density-matrix representation. This framework enables dynamic characterization of aligned and misaligned interbrain states and links these neural states to behavioral performance and empathic context, thereby grounding quantum formalism in testable neural mechanisms of social cognition.

Here, we recorded EEG from dyads during collaborative-memory and independent-memory encoding tasks (Fig. 1). Relative to independent encoding as a baseline, collaborative encoding exhibited higher aligned states within dyads, whereas misaligned states predominated during independent encoding. Based on these findings, we propose the Quantum Aligned-Misaligned Entanglement Model (QAEM), which captures stronger aligned and weaker misaligned states during collaboration relative to independent encoding. Interbrain entanglement further covaried with empathic responses, and its relationship with cooperative efficiency and memory performance depended on interpersonal context rather than stable traits. Together, these results suggest that quantum-inspired entanglement measures provide a neural index for characterizing connectivity between collaborating brains and establishes a neurophysiologically

grounded framework linking social neuroscience with quantum information theory.

Results

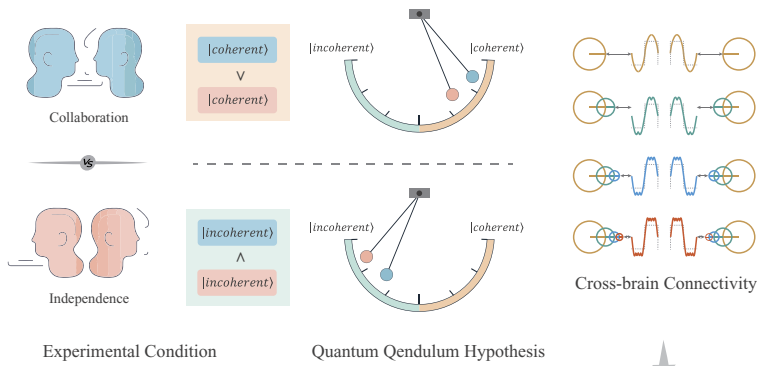
Collaborative Memory Encoding Demands More Cognitive Control Resources. In Experiment 1, we conducted simultaneous EEG recordings from 70 dyads (140 participants) using a 128-channel hyperscanning system during a memory encoding and recognition task (*Materials and Methods*). During encoding, participants judged the animacy of two-character words, followed by feedback and a brief intertrial interval (Fig. 2A). In the collaborative-condition (Colla), paired participants coordinated their response speed during word discrimination, with successful collaboration defined by reaction-time differences within a predefined threshold. In the independent-condition (Indep), participants performed the same task individually without response coordination. During subsequent recognition, participants classified words as novel or intact, engaging both familiarity- and recollection-based retrieval processes.

We first examined spontaneous collaboration rates and accumulative scores in the Indep using the predefined collaboration criterion (*Materials and Methods*). As expected, collaboration rates were significantly higher in the Colla than in Indep ($P < 0.0001$, Fig. 2B), accompanied by higher accumulative scores ($P < 0.0001$, Fig. 2C). To characterize neural differences during memory encoding, we analyzed task-related EEG activity. Relative to Indep, Colla elicited more negative N1 amplitudes associated with attentional allocation ($P < 0.0001$) and shorter P2 latencies reflecting increased cognitive control demands prior to behavioral responses. Because collaborative neural activity was confined to the stimulus presentation phase, we conducted source localization during this interval (*Materials and Methods*). Compared with Indep, Colla exhibited broader and stronger activation, with significant increases in the bilateral medial frontal cortex, anterior cingulate cortex, and superior temporal regions, indicating elevated cognitive resource demands during collaboration (Fig. 2G).

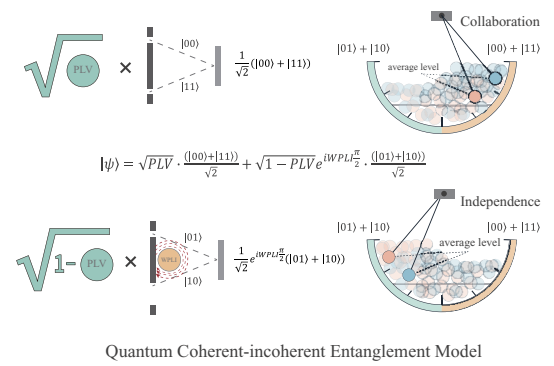
Behaviorally, reaction times were significantly shorter in Colla compared to Indep during encoding ($P = 0.002$, Fig. 2E) and retrieval phase ($P < 0.0001$, Fig. 2H). Accuracy was significantly lower in Colla during the retrieval phase ($P < 0.0001$). A similar pattern was observed in recollection-based retrieval, including significantly shorter reaction times ($P = 0.00095$) and lower accuracy ($P < 0.0001$, Fig. 2F) in Colla. Interestingly, familiarity-based retrieval revealed superior performance during collaboration, reflected in better accuracy ($P < 0.0001$) and shorter reaction times ($P < 0.0001$, Fig. 2I). Together, these results indicated that collaborative memory encoding demands more cognitive control resources, facilitating the familiarity-based retrieval processes.

Collaborative Brains Exhibit More Aligned States within the Quantum-Inspired Model. In this framework, the aligned state (|aligned>, AS) denotes greater consistency between two brains during collaborative-memory encoding, whereas the misaligned state (|misaligned>, MS) reflects reduced interbrain consistency. Accordingly, we hypothesized that collaborative encoding would be characterized by a higher probability of aligned states and a lower probability of misaligned states relative to independent encoding (Fig. 1A). To test this hypothesis, we analyzed dual-brain EEG signals acquired via hyperscanning (Fig. 1D) using the QAEM, which integrates PLV and WPLI as core neural indices (*Materials and Methods* and *SI Appendix*, Figs. S1 and S2 for model details).

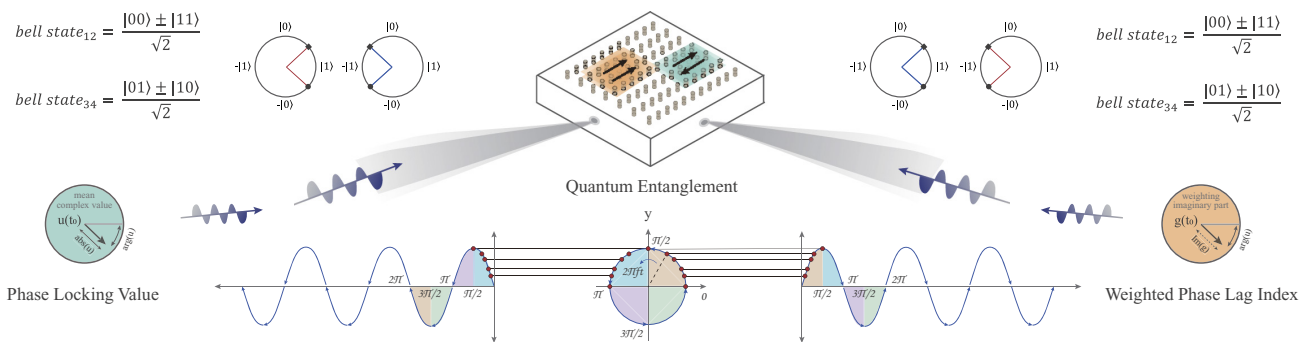
A Experimental Hypothesis



B Quantum Entanglement Model



C Quantum Entanglement Computation



D EEG Preprocessing

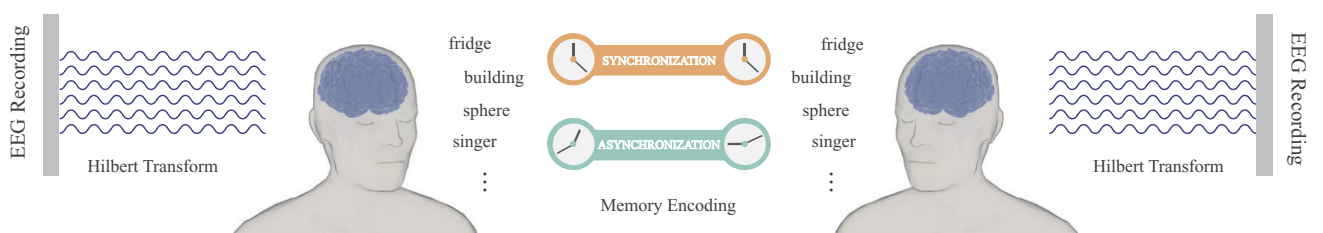


Fig. 1. Quantum cognitive framework for modeling interbrain entanglement during memory encoding. (A) Experimental hypothesis based on quantum alignment. Interbrain coordination is modeled as transitions between aligned and misaligned states under collaborative and independent encoding conditions. (B) In the QAEM, PLV governs the amplitude ratio between aligned and misaligned components, while WPLI introduces phase perturbation. These are combined in a dynamic quantum superposition to form the entangled state $|\psi\rangle$. This framework provides a principled method for translating neural synchrony into a bipartite quantum system for characterizing interbrain connectivity. (C and D) Schematic overview of the Quantum Aligned-Misaligned Entanglement Model (QAEM). Dual-brain EEG signals were recorded from participant dyads during collaborative or independent memory encoding tasks. Raw EEG recordings were bandpass filtered and transformed via the Hilbert method to extract instantaneous phases. Phase dynamics were compared across brains to evaluate interbrain synchronization, from which phase-locking values (PLV) and weighted phase lag indices (WPLI) were derived. These synchrony metrics were then used to parameterize the amplitude and phase of a two-qubit entangled system. Aligned and misaligned Bell states ($|00\rangle \pm |11\rangle$, $|01\rangle \pm |10\rangle$) served as basis states, modeling phase-consistent and phase-inconsistent interbrain configurations, respectively. The resulting entangled state $|\psi\rangle$ dynamically evolved based on neural coupling, capturing non-classical information sharing across brains.

We compared phase-locking value (PLV) between the Colla and Indep conditions during stimulus presentation across the 0 to 40 Hz frequency range (*SI Appendix, Fig. S3A*). Although PLV differences were observed across electrode pairs and cortical regions (*SI Appendix, Fig. S3A and B*), paired-sample *t* tests across dyads revealed no significant overall difference between conditions ($P = 0.227$, *Fig. 3B*). Source-level analyses similarly showed no statistically significant PLV differences between Colla and Indep, despite regional trends in temporal and parietal areas (*Fig. 3C and D* and *SI Appendix, Fig. S3F and G*). The relatively higher PLV observed in the temporal pole compared with the angular gyrus is consistent with prior work implicating anterior temporal regions in emotional processing, autobiographical memory, and episodic encoding within the default mode network (44). Collaborative-memory encoding requires joint recollection of

shared experiences, a process closely aligned with episodic memory formation, which has been shown to depend on coherent phase-based connectivity within medial and anterior temporal regions (3). In contrast, the angular gyrus, although involved in episodic and semantic memory through hippocampal-parietal circuits, has been characterized by predominantly directed rather than synchronized connectivity, suggesting a more passive role in information flow that may account for its lower PLV (45).

We observed lower PLV in the right inferior parietal cortex (parietal_Inf_R) than in the right precentral gyrus (precentral_R), consistent with previous reports (44, 46). The inferior parietal region, a core component of the default mode network, is primarily involved in spatial processing, episodic integration, and internally directed cognition, and has been characterized by localized, frequency-specific coupling rather than global synchronization

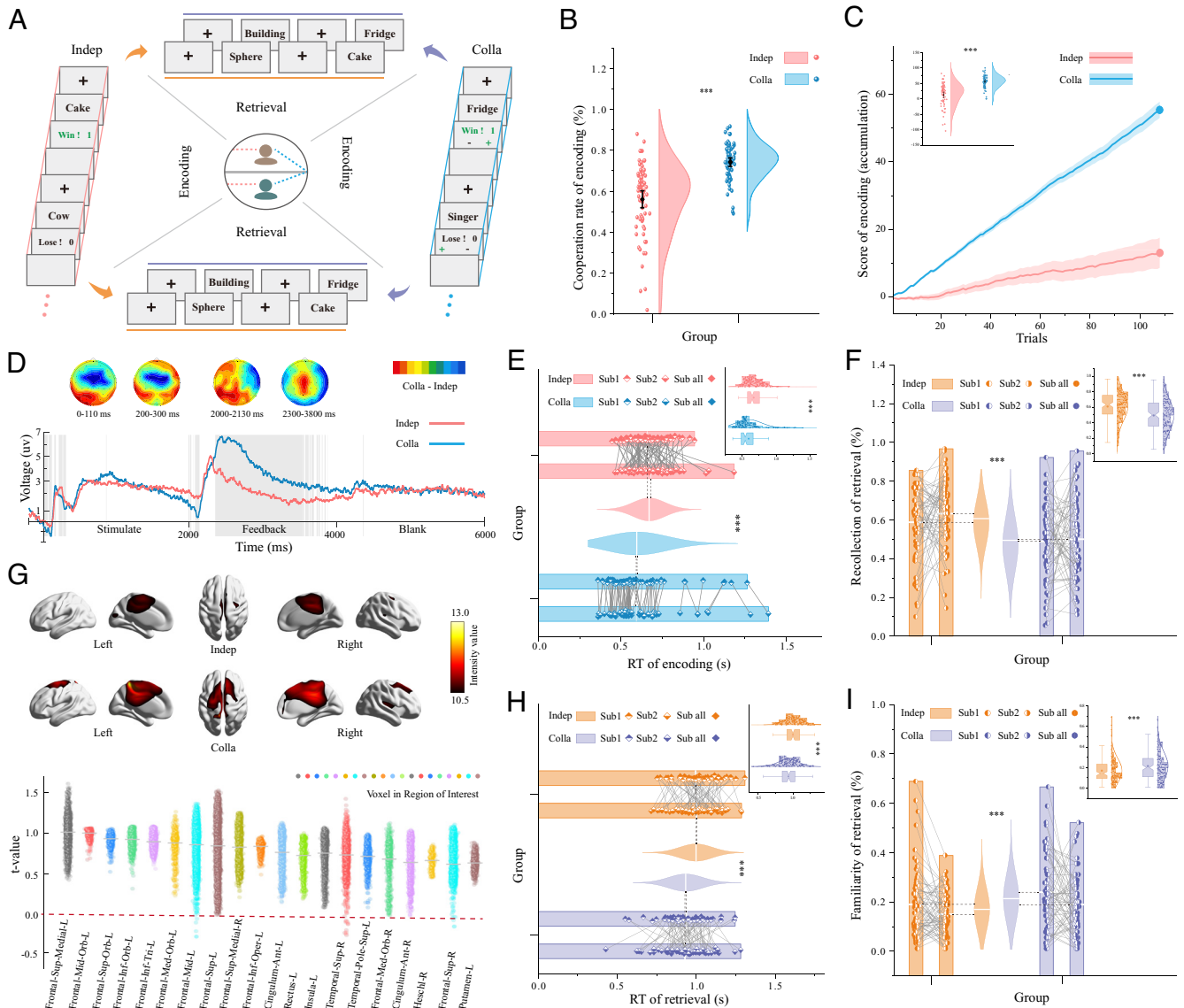


Fig. 2. Collaborative encoding engages greater cognitive control and supports familiarity-based retrieval. (A) Schematic of the experimental design. During encoding, dyads either performed animacy judgment tasks individually (Indep) or collaboratively by synchronizing response times (Colla). Memory was later tested via individual recognition judgments. (B) Collaboration rate was significantly higher in the collaborative condition. (C) Accumulative encoding scores increased more rapidly in the Colla condition across trials. (D) Grand-average ERP waveforms and topographies reveal enhanced attention-related N1 negativity and reduced P2 latency in the Colla condition during stimulus presentation, along with increased feedback-related negativity and feedback-related positivity following feedback onset. (E) Encoding reaction times were faster in Colla than in Indep. (F) Recollection-based retrieval showed shorter RTs but lower accuracy in Colla. (G) Source localization of stimulus-locked EEG activity revealed that collaborative encoding recruited a broader set of brain regions than independent encoding, including the medial superior frontal cortex, middle orbital frontal cortex, and superior orbital frontal cortex. (H) Retrieval RTs were shorter in Colla. (I) Familiarity-based retrieval demonstrated both higher accuracy and faster RTs following collaborative encoding. Error bars and shaded regions denote \pm SEM; $**P < 0.001$. Topographies show difference waves (Colla – Indep). All statistics are from paired *t* tests unless otherwise specified.

(44, 47). In contrast, the precentral gyrus (motor cortex) exhibits stronger global phase synchronization during task performance, reflecting its role in motor control and coordination (44). This distinction between localized parietal synchronization and globally coordinated motor activity provides a parsimonious explanation for the lower PLV observed in parietal_Inf_R during collaborative tasks (44–46).

Analyses of the weighted phase lag index (WPLI) revealed robust differences between conditions, with significantly higher interbrain WPLI in the Indep than in the Colla (Fig. 3E and SI Appendix, Fig. S4 A and B). Paired-sample tests across dyads confirmed that positive WPLI differences favored Indep over Colla ($P < 0.0001$; Fig. 3F). Source-level analyses further showed more widespread regions exhibiting elevated WPLI in Indep, whereas no cortical region displayed higher WPLI in Colla (Fig. 3 G and

H and SI Appendix, Fig. S4F). The strongest difference was observed in the right superior occipital gyrus ($P = 0.036$; Fig. 3H). These findings indicate that interbrain synchronization captured by WPLI is enhanced during independent encoding, likely reflecting shared stimulus processing rather than genuine interpersonal coupling, which is reduced during collaboration.

The contrasting PLV and WPLI results reflect fundamental differences between these metrics. PLV captures phase coherence irrespective of phase lag and includes zero-lag synchronization, making it sensitive to shared stimulus-driven responses, whereas WPLI emphasizes consistent non-zero-lag coupling and suppresses instantaneous correlations (48, 49). Accordingly, no significant PLV differences emerged between collaborative and independent encoding, whereas WPLI revealed stronger interbrain synchronization in the independent condition. This pattern likely reflects

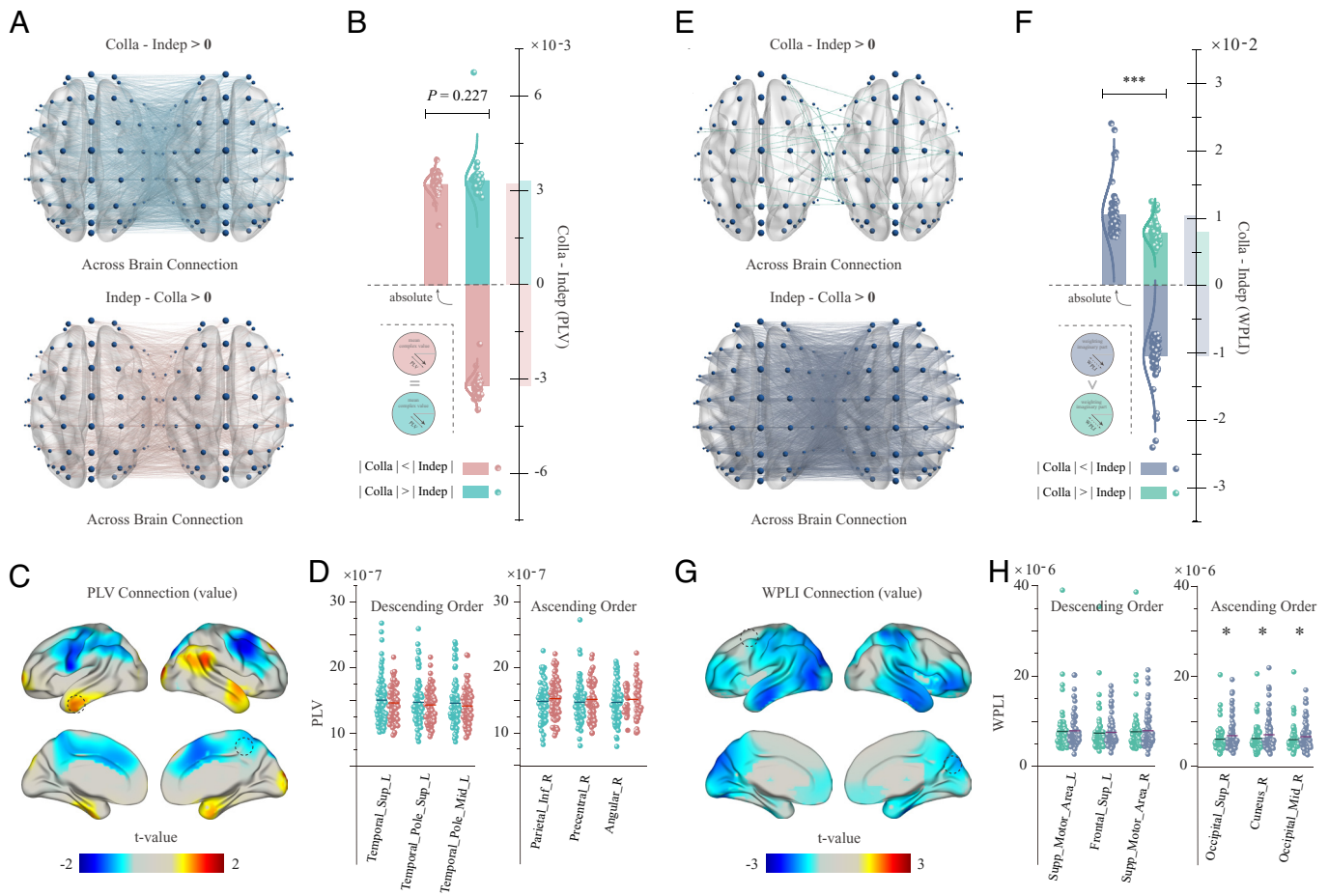


Fig. 3. Comparisons of interbrain phase synchrony (PLV) and phase-lag connectivity (WPLI) between collaborative and independent encoding. (A) Visualizations of cross-brain PLV connectivity patterns corresponding to Colla > Indep (Top) and Indep > Colla (Bottom). (B) Paired-sample *t* test comparing the absolute PLV difference across dyads revealed no significant group-level difference. (C) Source-level paired *t*-map showing voxel-wise differences in PLV (Colla - Indep) during encoding. (D) Mean PLV values across ROIs (AAL-90 atlas), sorted by descending and ascending *t*-values of Colla - Indep comparisons, respectively. (E) Visualizations of cross-brain WPLI connectivity patterns corresponding to Colla > Indep (Top) and Indep > Colla (Bottom). (F) Paired-sample *t* test comparing the absolute WPLI difference across dyads revealed a significant group-level effect. (G) Source-level paired *t*-map showing voxel-wise differences in WPLI (Colla - Indep) during encoding. (H) Mean WPLI values across ROIs (AAL-90 atlas), sorted by descending and ascending *t*-values of Colla - Indep comparisons, respectively.

shared sensory processing during independent encoding, in which participants viewed identical stimuli and engaged in similar encoding operations, yielding stable phase-lagged coupling captured by WPLI. Consistent with this interpretation, regions showing the largest WPLI differences were primarily located in the occipital cortex (SI Appendix, Fig. S4 F and G), supporting a dominant contribution of early visual processing rather than genuine interpersonal coupling (45, 47, 50–52).

Consistent with our hypothesis, the Quantum Aligned-Misaligned Entanglement Model revealed significantly higher aligned-state (AS) probabilities during Colla than Indep encoding (Fig. 4A and SI Appendix, Fig. S5 A and B). Paired-sample analyses confirmed that average AS probabilities were significantly elevated in Colla relative to Indep ($P = 0.0001$; Fig. 4B). Source-level analyses further demonstrated higher AS probabilities across cortical regions in Colla, with no region showing greater AS probability in Indep (Fig. 4 C and D and SI Appendix, Fig. S5 F and G). These findings indicate that increased aligned entanglement characterizes collaborative memory encoding and supports AS probability as a neural signature of interbrain connectivity during cooperation. In contrast to the PLV-based results (Fig. 3), AS probabilities derived from QAEM showed a distinct spatial pattern, with nearly all regions exhibiting higher AS probabilities during Colla than Indep

encoding (Fig. 4). Notably, the strongest Colla > Indep differences were observed in the occipital cortex rather than in temporal regions, consistent with the visual demands of the collaborative task, which required coordinated responses to shared visual stimuli. As a primary locus of early visual processing and attention modulation, the occipital cortex is well positioned to support enhanced cross-brain alignment during joint visual monitoring, accounting for its elevated AS probabilities under collaborative conditions (50, 53).

In contrast to aligned states, misaligned-state (MS) probabilities showed the opposite pattern across conditions. MS probabilities were significantly higher during Indep than Colla encoding at both sensor and source levels (Fig. 4 E–G and SI Appendix, Fig. S6 A and B). Paired-sample analyses confirmed that average MS probabilities were significantly reduced in Colla relative to Indep ($P < 0.0001$; Fig. 4F), with no cortical region exhibiting higher MS probabilities during collaboration (Fig. 4H and SI Appendix, Fig. S6 F and G). Regions showing the strongest Indep > Colla effects were primarily located in visual and occipital cortices, indicating more widespread cross-brain inconsistency during independent encoding. These findings are consistent with the interpretation of MS as reflecting divergent interbrain dynamics, which are attenuated during collaboration through shared cues and coordinated processing.

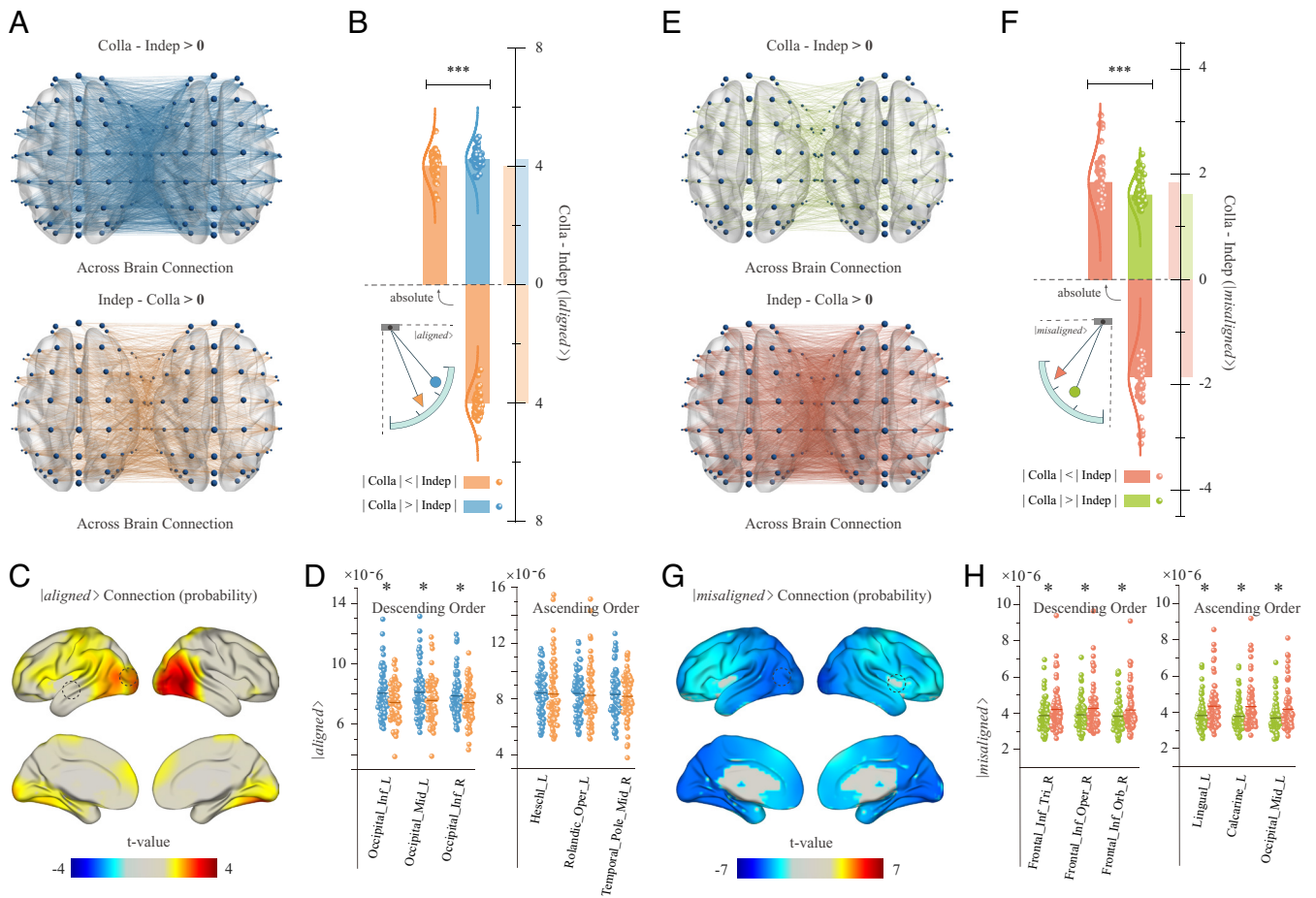


Fig. 4. Comparisons of interbrain aligned and misaligned quantum states between collaborative and independent encoding. (A) Interbrain connectivity maps visualize AS probability differences between conditions, with denser cross-brain connections observed for Colla (Top). (B) Group-level paired *t* test revealed significantly higher average AS probabilities in Colla than in Indep. (C) Voxel-wise statistical maps indicate that Colla elicited higher AS probabilities in widespread cortical regions, especially the bilateral occipital cortices. (D) Regional analysis of AS probabilities across AAL-90 ROIs confirmed significantly higher values for Colla in all regions, with the largest effect observed in the left inferior occipital gyrus. No brain regions exhibited significantly higher AS probabilities in the Indep condition. (E) Interbrain connectivity maps visualize denser and more widespread misaligned-state connections in the Indep condition. (F) Group-level paired *t* test confirms significantly higher average MS probabilities in Indep than in Colla. (G) Voxel-wise statistical maps reveal elevated MS probabilities across broad cortical areas in the Indep condition, especially in frontal and occipital regions. (H) ROI-based comparisons ranked by Δ MS (Colla – Indep) *t*-values show consistently greater MS probabilities in the Indep condition across all regions.

Individual Difference Predictors of Interbrain Alignment and Misalignment. Interbrain entanglement states formed during collaborative encoding selectively predicted familiarity-based retrieval and exhibited task-phase-specific neural dynamics (SI Appendix, Supplementary Results), motivating our subsequent investigation of individual differences underlying interbrain alignment and misalignment. To examine how individual differences modulate interbrain alignment, we assessed three psychological constructs: Inherent Empathy (IE), Interpersonal Affinity Change (IAC), and Social Cognitive Disposition (SCD). IE and IAC capture general interpersonal tendencies that influence alignment across both collaborative and independent conditions and therefore cannot explain the collaboration-specific increase in AS probability. To isolate alignment uniquely induced by collaboration, SCD was quantified as the contrast between collaborative and independent AS probabilities ($AS_{colla} - AS_{indep}$) across task phases. Correlation analyses were conducted separately for IE and IAC within each condition and for SCD using the collaborative-independent contrasts, with false discovery rate correction applied within each construct. The same analytical framework was applied to MS probabilities.

After Benjamini–Hochberg correction, significant associations between IE and AS probabilities were observed only during the

blank phase, and this effect was consistent across Colla and Indep conditions ($r_{colla} = 0.227$, $P_{colla} = 0.048$, $r_{indep} = 0.285$, $P_{indep} = 0.048$, Fig. 5C and SI Appendix, Fig. S6C). This pattern indicates that IE reflects a task-independent propensity for spontaneous interbrain alignment that emerges in the absence of external stimulation. No FDR-corrected IE effects were observed during stimulus or feedback phases, where task-related demands likely dominate neural activity. Accordingly, IE cannot account for the increased AS probability observed during collaborative encoding, motivating our subsequent analysis of SCD to identify individual factors specifically associated with collaboration-induced alignment.

SCD was significantly associated with collaboration-induced changes in interbrain states during task engagement. During the Stimulate phase, higher SCD scores (poorer attention switching) were linked to reduced Colla-Indep gains in AS, whereas lower SCD scores predicted the opposite pattern (Fig. 5). In contrast, SCD scores were significantly associated with Colla-Indep gains in MS during both the Stimulate and Feedback phases (SI Appendix, Fig. S11). No significant SCD effects were observed during the Blank phase. These complementary AS and MS results indicate that attention-switching capacity selectively modulates collaboration-induced neural alignment, promoting a shift from misalignment toward alignment during phases requiring active external

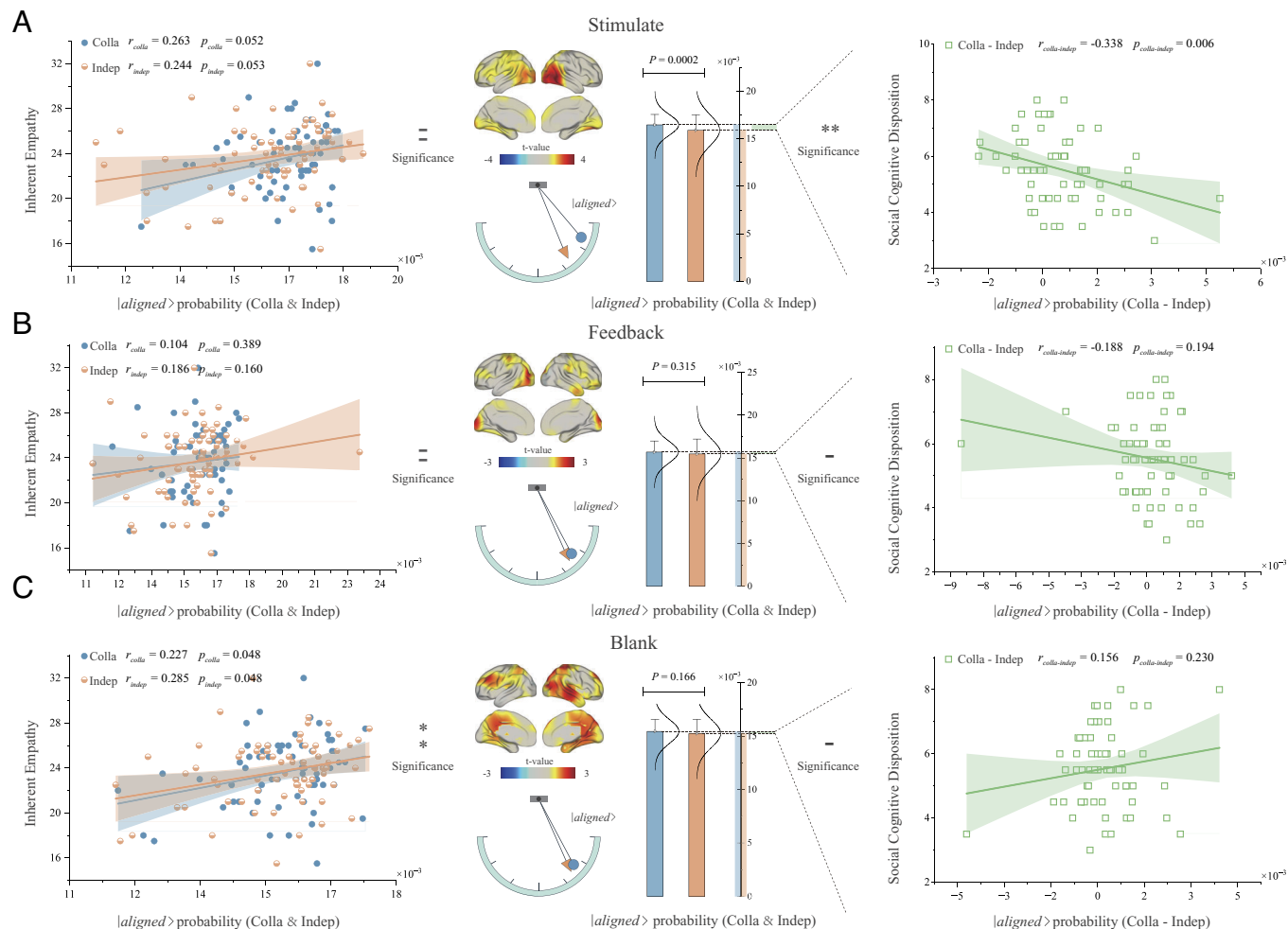


Fig. 5. Individual-difference predictors of interbrain aligned-state (AS) dynamics across task phases. Each row corresponds to one task phase: (A) Stimulate, (B) Feedback, and (C) Blank. Within each phase, the panels from *Left to Right* show. *Left panels* Correlation between AS probability and Inherent Empathy (IE), shown separately for the collaborative (Colla, blue) and independent (Indep, orange) conditions. Scatterplots display individual data points and regression fits. Reported P -values are FDR-corrected within the IE family (six tests). *Middle panels* Group-level comparison of AS probabilities between the Colla and Indep conditions. Brain surface maps display ROI-level t -values. The adjacent gauge diagram illustrates the overall direction of group differences. Bar plots compare mean AS probabilities between conditions using paired-sample t tests. *Right panels* Correlation between SCD (attention-switching dimension of ASQ) and the Colla - Indep difference in AS probability. Scatterplots represent individual difference scores along with regression fits. Reported P -values are FDR-corrected within the SCD family (three tests). Together, the three sets of analyses dissociate trait-like alignment tendencies (IE), task-induced differences between collaborative and independent encoding, and individual variability in collaborative alignment gains predicted by attention-switching ability (SCD).

information processing ($r_{colla-indep} = -0.338$, $P_{colla-indep} = 0.006$, Fig. 5A and $r_{colla-indep} = 0.345$, $P_{colla-indep} = 0.009$, SI Appendix, Fig. S11). Frequency-specific analyses revealed complementary roles of theta and beta bands. In the theta band (2 to 10 Hz), collaboration primarily modulated the MS, with increased MS during the Stimulate phase and positive associations between SCD and collaboration-induced MS changes, particularly among individuals with poorer attention switching. In contrast, beta-band activity (12 to 20 Hz) predominantly modulated the AS, with collaboration enhancing AS during the Stimulate phase and SCD reliably predicting AS gains across task phases, such that better attention switching was associated with stronger alignment. These frequency-specific patterns extend the broadband findings, with detailed statistics provided in SI Appendix, Tables S1–S6.

Empathy Training Selectively Modulates Interbrain Quantum States during Cooperative Memory Encoding. In Experiment 1, mediation and moderation analyses further suggested that empathy may modulate the relationship between cooperative behavior, interbrain quantum states, and memory performance, although these effects were inherently correlational in nature (SI Appendix,

Fig. S14). To test whether interbrain quantum states are modulated by interpersonal context rather than stable traits alone, we conducted Experiment 2, which incorporated an empathy enhancement training prior to the cooperative memory task (SI Appendix). Using the same paradigm and entanglement framework as in Experiment 1, we examined aligned and misaligned state probabilities across task phases before and after training. Following empathy training, the differentiation between collaborative-memory and independent-memory encoding observed during the stimulation phase was selectively attenuated, with no significant Colla-Indep differences in misaligned states and a reduced difference in aligned states (SI Appendix, Table S8). These results indicate that enhancing empathic context can causally modulate interbrain quantum states during cooperative memory encoding.

Fig. 6 summarizes the effects of empathy training on interbrain entanglement states and behavior during cooperative encoding. Prior to training, Colla encoding deviated from the Indep baseline, exhibiting altered interbrain entanglement distributions and reduced memory accuracy during the stimulation phase. Following empathy training, entanglement state probabilities under Colla converged toward the Indep baseline, accompanied by a recovery

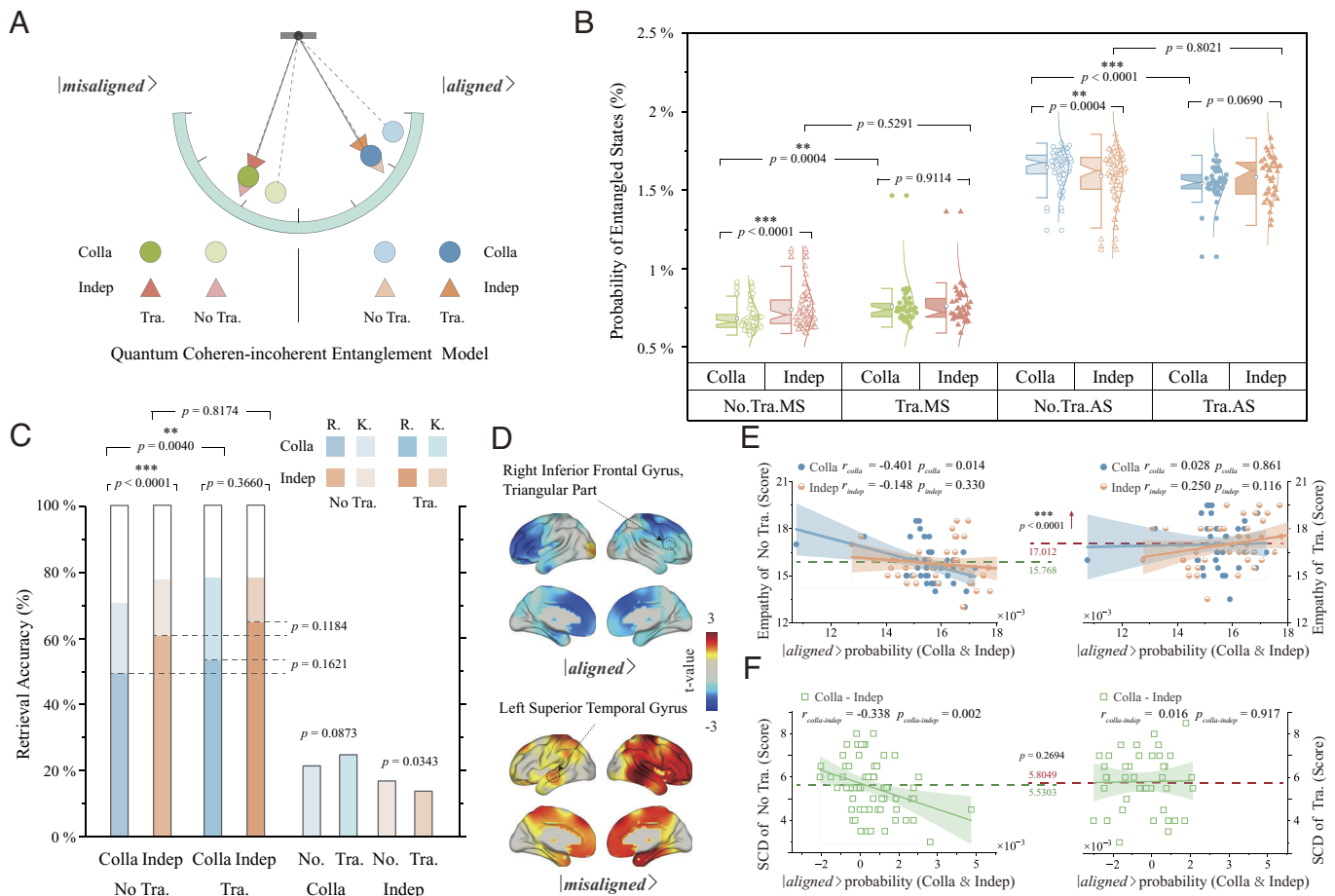


Fig. 6. Empathy training reshapes interbrain entanglement dynamics and behavioral outcomes during cooperative encoding. (A) Conceptual illustration of the Quantum Aligned-Misaligned Entanglement Model, with independent encoding (Indep) serving as the baseline. Empathy training is hypothesized to reduce additional coordination-related cognitive demands during collaboration (Colla), leading to a return toward baseline entanglement distributions. (B) During the stimulus phase, Colla shows increased $|aligned\rangle$ and reduced $|misaligned\rangle$ probabilities relative to Indep before training, whereas these differences are attenuated after empathy training. (C) Behavioral results mirror neural patterns, with reduced retrieval accuracy for Colla relative to Indep before training and comparable performance after training. (D) Source-level contrasts reveal a shift in Colla-Indep entanglement differences from occipital regions before training to social-cognitive regions after training. (E and F) Empathy training increases situational empathy and alters the associations between interbrain alignment, empathic responses, and attention switching.

of collaborative memory performance (Fig. 6 B and C). At the spatial level, empathy training altered the cortical distribution of Colla-Indep differences, shifting entanglement-related effects from occipital visual regions toward frontal and temporal areas associated with social cognitive processing (Fig. 6D). Together, these results indicate that empathy training normalizes both neural coupling patterns and behavioral outcomes during cooperative memory encoding.

To assess how empathy training reshapes individual influences on interbrain entanglement during cooperative encoding, we examined both situational empathy and stable traits (SI Appendix). Empathy training significantly increased situational empathy scores (SES-CC; Fig. 6E). Before training, AS probabilities during cooperation were correlated with situational empathy, whereas this relationship was no longer present after training, indicating a decoupling of entanglement states from subjective empathic variation. Similarly, prior to training, collaboration-induced AS differences (Colla-Indep) were associated with attention-switching ability, but this association was abolished following training (Fig. 6F). Together, these results indicate that empathy training reduces the influence of stable traits on interbrain entanglement, rendering neural alignment during cooperative encoding more sensitive to immediate social context than to enduring individual differences.

Discussion

This study demonstrates that quantum-inspired interbrain entanglement measures provide a principled means of distinguishing collaborative-memory from independent-memory encoding, even in the absence of explicit behavioral coordination or direct signal exchange, thereby overcoming ambiguities inherent to traditional synchrony-based approaches. Collaborative-memory encoding was characterized by increased probabilities of aligned states and reduced misaligned states, reflecting enhanced interbrain consistency, whereas independent encoding showed greater neural divergence. Consistent with this dissociation, aligned-state probabilities selectively mediated the facilitation of familiarity-based retrieval during collaboration, whereas independent encoding engaged neural mechanisms supporting both familiarity and recollection. Importantly, interbrain entangled states were dynamic and context dependent, evolving across task stages and covarying with situational empathic engagement. Together, these findings suggest that interbrain entanglement captures flexible interpersonal coordination mechanisms that link social interaction with memory outcomes and may generalize to other cooperative domains requiring shared timing and mutual adjustment, such as musical performance.

Quantum-Inspired Interbrain Coupling beyond Neural Synchrony. Recent work on interbrain synchrony (IBS) highlights the role of synchronized neural activity in social interaction and coordination (54–56), yet the field remains limited by conceptual ambiguity and methodological challenges, particularly the difficulty of dissociating genuine interbrain connectivity from stimulus-driven entrainment, motor artifacts, or attentional confounds (57–59). Moreover, the functional and causal significance of IBS remains debated, as most evidence is correlational rather than mechanistic (55, 56). In this context, our study introduces a quantum entanglement–based framework that extends classical synchrony models by capturing interbrain connectivity beyond oscillatory phase alignment. Unlike conventional IBS metrics, quantum entanglement formalizes nonlocal correlations in neural dynamics (60, 61), consistent with principles from quantum information theory demonstrating robust coherence across spatial separation (62). By characterizing aligned and misaligned entanglement states during memory encoding, we show that interbrain entanglement provides a functionally distinct index of connectivity that cannot be fully explained by classical synchrony alone (17, 63, 64). The predominance of aligned states during collaboration and their association with enhanced familiarity-based retrieval further support a role for entanglement in interbrain integration (58), in line with theoretical work linking entangled states to improved learning and adaptive optimization (65, 66). To formalize this distinction, we propose the QAEM framework, which embeds quantum-inspired entanglement within a structured account of interbrain coordination, mitigating spurious synchrony effects and offering a conceptual bridge between classical synchronization and quantum-inspired modeling approaches (67–69). Although the QAEM is derived from cortical phase relations, the model does not presuppose a specific physiological source for these dynamics. Subcortical generators, such as hippocampal or thalamocortical inputs, can shape cortical rhythms within each individual, yet their influence is inherently integrated into the probabilistic mixture of $|aligned\rangle$ and $|misaligned\rangle$ states. At the current level of abstraction, the model does not attempt to disentangle specific neural generators, but instead focuses on their collective impact on interbrain coordination. As a result, the quantification of interbrain alignment reflects the emergent coordination between two cortical systems, regardless of whether upstream drivers arise from cortical or subcortical pathways.

Across the four neural indices examined, the ROI-level patterns converge on a coherent neurophysiological account that aligns with established findings in human memory research. For PLV, collaborative encoding elicited relatively higher phase coherence in anterior temporal regions than in angular or inferior parietal areas, consistent with evidence that temporal pole regions contribute preferentially to episodic and socially contextualized memory, whereas inferior parietal regions exhibit more localized and task-dependent coupling rather than global synchronization (3, 44–47). In contrast, WPLI revealed consistently higher values during independent encoding across occipital, parietal, and temporal regions, suggesting more stable, stimulus-driven phase-lagged coupling when participants encode information independently, without the added variability introduced by mutual adjustment during collaboration (48, 49). The entanglement-based measures revealed complementary patterns. Aligned-state (AS) probabilities were elevated during collaborative encoding across occipital, angular, and temporal regions, consistent with enhanced cross-brain consistency arising from shared visual input and coordinated cognitive engagement. Conversely, misaligned-state (MS) probabilities were higher during independent encoding, particularly in occipital and parietal cortices, suggesting greater divergence in

visual and spatial processing when individuals rely on idiosyncratic strategies and fluctuating attention (51). Together, these convergent patterns across PLV, WPLI, AS, and MS suggest that collaborative and independent encoding recruit distinct large-scale network dynamics, in close agreement with the broader electrophysiological literature on memory and social cognition.

Frequency-resolved ROI analyses further clarified the neural systems supporting collaborative encoding. In the theta band (*SI Appendix, Table S5*), the strongest AS-MS differences were localized to fronto-parietal regions, including the superior parietal lobule, inferior frontal gyrus, and angular gyrus, areas long associated with shared attention, semantic integration, and episodic binding (44, 51, 52). Their prominence in theta oscillations aligns with the well-established role of theta-band activity in coordinating large-scale mnemonic networks and socially guided encoding. In contrast (*SI Appendix, Table S6*), beta-band effects showed a more selective organization: collaboration-related increases in AS were concentrated in left angular, middle temporal, and superior parietal regions, consistent with beta's involvement in semantic unification and schema-dependent memory processes (47, 53). Meanwhile, MS effects were dominated by orbitofrontal and supplementary motor areas, regions previously implicated in conflict monitoring and coordination demands during joint tasks (3, 45). Together, these frequency-specific patterns complement the broadband results by demonstrating that theta oscillations index broad attentional and integrative demands of collaboration, whereas beta oscillations differentiate representational alignment from coordination-related divergence.

Quantum-Inspired Entanglement Links Collaborative Encoding to Memory Retrieval. Collaborative memory encoding has been shown to enhance familiarity-based retrieval, as social interaction and shared attention facilitate fluency and mutual reinforcement in information processing (70). Our findings are consistent with this perspective, demonstrating that $|aligned\rangle$ occur more frequently during collaboration and are associated with enhanced familiarity-based retrieval performance, linking cooperative encoding fluency to subsequent memory outcomes, whereas $|misaligned\rangle$, which dominate in independent encoding, predict both familiarity-based and recollection-based retrieval. The probability of entangled states further supports this pattern, as collaborative encoding led to a higher occurrence of $|aligned\rangle$, while independent encoding was associated with a greater presence of $|misaligned\rangle$. This suggests that $|aligned\rangle$ reflect heightened interbrain consistency, stabilizing neural representations, whereas $|misaligned\rangle$ indicate greater neural inconsistency, requiring broader information integration. The absence of $|aligned\rangle$ probability differences after encoding reinforces the idea that interbrain consistency is a function of collaborative encoding rather than postencoding processes. However, the persistence of higher $|misaligned\rangle$ probabilities in independent encoding suggests lingering effects of reduced synchronization.

Quantum memory models provide a theoretical basis for these findings. Quantum probability frameworks suggest that memory retrieval can be described as a process analogous to state collapse from a mixed state, where the interplay between coherence and entanglement influences retrieval outcomes (28, 71). Our findings suggest that $|aligned\rangle$ during collaborative encoding reflect a higher proportion of effective coherence, stabilizing neural representations and facilitating rapid retrieval (72). In contrast, $|misaligned\rangle$ may correspond to entanglement-driven fluctuations, supporting broader information integration and more flexible retrieval (40). The disappearance of differences in entangled states when no stimuli or feedback were presented further supports this

interpretation, indicating that the encoding phase determines the connectivity structure. These results align with studies on entangled-state learning complexity, which suggest that an adaptive balance between coherence and entanglement optimizes retrieval mechanisms (27, 73). Together with structural modeling results, these findings reinforce the mechanistic validity of the QAEM framework, in which quantum-inspired entangled states dynamically mediate the transformation from cooperative neural alignment to behavioral memory enhancement.

State-Dependent Modulation of Interbrain Alignment during Cooperative Encoding. Empathy contributes to collaborative efficiency by modulating interbrain dynamics during social interaction, with neural synchrony reflecting not only stable individual dispositions but also sensitivity to the immediate interpersonal context (74, 75). Our findings refine this perspective by showing that the relationship between empathy and interbrain alignment is context dependent rather than uniformly trait driven. In the absence of empathy training, individual differences in empathic traits were associated with variations in aligned-state probability during collaborative encoding, whereas this relationship was not observed during independent encoding. Following empathy training, these trait-based associations were no longer evident, indicating that interbrain alignment is not a fixed neural disposition but can be reshaped by changes in the interpersonal context. In parallel, situational empathy exhibited a dynamic relationship with aligned-state occurrence during cooperation prior to training, a pattern that was altered after the intervention. Together, these findings suggest that [aligned] states reflect a flexible neural mode of interpersonal coordination that is sensitive to both momentary social engagement and task demands, rather than a stable marker of inherent interpersonal synchrony (76, 77). In QAEM, [aligned] states can be conceptualized as a context-sensitive mode of interbrain coordination, reflecting the momentary coupling between interacting individuals rather than a stable, trait-bound synchrony mechanism. Empathy, therefore, does not rigidly determine neural alignment but modulates the conditions under which aligned interbrain states are more likely to emerge during cooperative engagement (16, 78). Related work in complex systems and network dynamics further supports this, as coherence has been shown to enhance collective coordination in distributed systems (27, 60). The persistence of [aligned] states during collaborative encoding, together with their sensitivity to empathic engagement and social interaction context, suggests that these states index a flexible neural mode of interpersonal coordination rather than a marker for fixed individual capacity.

From Behavioral Analogies to Neural Evidence. Quantum cognition research has long been devoted to exploring nonclassical structural dependencies in human cognition (28), with particular interest in how “entanglement” may account for nonlinear phenomena in judgment, learning, and decision-making. Within this theoretical framework, most existing studies have attempted to construct specific behavioral paradigms or experimental scenarios to indirectly simulate or analogically infer the presence of entanglement-like structures within individual cognitive systems [for example, some studies have hypothesized mental connections between monozygotic twins and constructed entanglement-based stimulus materials to investigate synchronized effects in implicit learning (43); other studies have applied quantum probabilistic models to behavioral data and analyzed the correspondence between model parameters and hemodynamic brain signals (38)].

In contrast, the present study fundamentally extends this paradigmatic path. We empirically characterized interbrain coupling

within a quantum-inspired modeling framework during cooperative interaction, using dual-brain EEG hyperscanning and neural synchrony indices as the foundational signal basis. Importantly, our approach is not grounded in notions such as telepathy, consciousness linkage, or other metaphysical constructs; rather, it is built upon measurable neural synchrony and grounded in empirically observable brain dynamics. Using the QAEM, we derived effective interbrain coupling states from dual-EEG recordings acquired during cooperative memory encoding and showed that these states systematically covaried with familiarity-based memory performance. Rather than constituting a fixed predictive pathway, the relationship between interbrain coupling, cooperative efficiency, and behavioral outcomes was found to depend on the interpersonal context in which cooperation unfolded. Individual differences in empathy were associated with variations in these relationships prior to training, but such associations were attenuated following empathy enhancement, indicating that interbrain coupling reflects a context-sensitive coordination process rather than a stable trait-dependent mediator. Future work may extend the present framework by incorporating higher-dimensional and multiscale neural representations, allowing a more fine-grained characterization of interbrain coordination beyond the current binary, coarse-grained formulation.

Materials and Methods

Participants. Experiment 1. Seventy-three dyads (146 participants) underwent simultaneous EEG hyperscanning. Three dyads were excluded due to technical issues or failure to complete the task, yielding a final sample of 70 same-sex dyads (30 male dyads; age 18 to 30 y, $M_{\text{age}} = 21.721$ y, $SD_{\text{age}} = 2.414$ y), all included in behavioral and neural analyses., all were included in behavioral and neural analyses. Experiment 2. Forty-two dyads were recruited for the empathy training experiment (*SI Appendix, Empathy Enhancement Training and Related Measures*). One dyad was excluded due to incomplete participation, resulting in a final sample of 41 dyads (16 male dyads; age range: 18 to 30 y; $M = 23.195$, $SD = 2.526$), all included in subsequent analyses.

All participants reported normal or corrected-to-normal vision and no history of neurological or psychiatric disorders. Participants received monetary compensation (\$14 base payment plus performance-based bonuses, totaling \$15-19). All procedures were approved by the Institutional Review Board of the School of Psychology, Capital Normal University, China (Ethics Approval No. CNU-20230902), and conducted in accordance with the Declaration of Helsinki. Written informed consent was obtained prior to participation, and participants were informed of their right to withdraw without penalty.

Task and Procedure. In each dyad, two same-sex strangers (Sub1 and Sub2) were briefly introduced and seated on opposite sides of a table, separated by a partition to prevent visual contact (Fig. 2A). Stimuli were presented on monitors, and responses were recorded via keyboards. The experiment consisted of encoding and retrieval sessions. During encoding, participants completed collaborative and independent tasks in a counterbalanced order, with three blocks per task (108 trials total). During retrieval, participants performed a word recognition task including items from both encoding conditions, comprising six blocks (360 trials total). All tasks were implemented using PsychoPy 2023.2.3. In both experiments, participants completed the Interpersonal Reactivity Index (IRI) to assess trait empathy and rated their partner before and after the session to index changes in interpersonal perception. In Experiment 1, participants additionally completed the Autism Spectrum Quotient (ASQ) prior to task performance. In Experiment 2, following empathy enhancement training, participants completed the Situational Empathy Scale for Cooperative Contexts (SES-CC) and the ASQ to assess state-dependent empathy and attentional switching. Detailed descriptions of questionnaire measures are provided in the *SI Appendix*.

Collaborative task. Each trial began with a fixation cross (900 to 1,100 ms), followed by a two-character word presented for 2,000 ms (Stimulate screen; Fig. 2A). Participants judged whether the word denoted an animate or inanimate entity and responded simultaneously with their partner using designated keys

(Sub1: F/J; Sub2: D/K). To prevent auditory cues, participants wore earplugs, and no verbal or physical communication was permitted. A successful collaboration was defined when the response-time difference between partners was smaller than a predefined threshold, $T = (RT_1 + RT_2)/8$, yielding one point for both participants; otherwise, each lost one point. This threshold was selected to maintain moderate task difficulty (79). Following each response, a 2,000-ms feedback screen displayed the outcome, cumulative score, and relative response speed, followed by a 2,000-ms blank intertrial interval. Each block consisted of 36 trials (approximately 252 s per block).

Independent task. The independent task followed the same procedure as the collaborative task (Fig. 2A), except that participants performed the task individually without coordination, and the feedback screen displayed only the outcome and cumulative score, without response-speed information.

Word recognition tasks. Participants completed an individual word recognition task including items from both encoding conditions. Each trial began with a fixation cross (900 to 1,100 ms), followed by a two-character word presented for 2,000 ms. Participants classified each word as *Remember* (R; recalled with contextual details), *Know* (K; familiar without context), or *New* using designated keys (D/F/J, respectively). No feedback was provided during recognition.

Dual-Brain EEG Data Acquisition. EEG data were simultaneously recorded from both participants in each dyad using a 128-channel hyperscanning system (SynAmps2, NeuroScan; 64 channels per participant; passband: 0.01 to 100 Hz; sampling rate: 1,000 Hz). Dual EEG streams were synchronized via triggers delivered through a central server computer. Signals were acquired from 64 scalp electrodes positioned according to the international 10-10 system, with M1 as the reference and electrode impedances maintained below 10 k Ω . Visual stimuli were presented concurrently on separate monitors synchronized to the same server. Electrooculographic (EOG) signals were recorded to monitor eye movements and ocular artifacts.

EEG Data Analysis. EEG preprocessing was performed using EEGLAB. Continuous data were bandpass filtered (0.1 to 40 Hz), rereferenced to the average of M1 and M2, and cleaned using independent component analysis to remove ocular, cardiac, and muscle artifacts. Data were visually inspected, and epochs exceeding ± 100 μ V were rejected. EEG signals were segmented into stimulus, feedback, and blank periods; for the collaborative condition, only successfully coordinated trials were retained. To reduce volume conduction effects, current source density (CSD) transformation was applied using the CSD Toolbox, and phase-based inter-brain connectivity metrics (PLV and WPLI) were computed from CSD-transformed signals. To isolate non-phase-locked oscillatory activity, trial-averaged event-related potentials were removed prior to connectivity and entanglement analyses, following established procedures (80). Source-level analyses, including inverse modeling and searchlight-based clustering, were conducted using FieldTrip, with surface-based visualization performed in BrainNet Viewer. Quantum cognitive modeling of EEG signals was implemented in MATLAB (R2019a, MathWorks).

Quantum Cognitive Model. In the quantum cognitive model, phase-locking value (PLV) and weighted phase lag index (WPLI) were used to quantify interbrain phase relationships. PLV captures the stability of instantaneous phase differences and has been widely used to index large-scale cortical coordination across cognitive states, with refined formulations improving robustness to noise and volume conduction (48, 81, 82). WPLI complements PLV by emphasizing consistent non-zero phase lags while suppressing spurious synchrony, providing a principled estimate of structured phase variability in neural networks (48). These properties align with formal treatments of phase coherence and decoherence in quantum information theory (83, 84) and have demonstrated reliability in applied EEG contexts, including behavioral decoding and sleep-related network analyses (85, 86). Within the QAEM framework, PLV determines the amplitude weighting of the aligned component of the quantum state, whereas WPLI modulates the phase structure of the misaligned component, jointly enabling neural instantiation of entanglement dynamics. Detailed theoretical justification is provided in the *SI Appendix*.

To characterize the dynamic interbrain relationship during collaborative memory encoding, we developed a quantum-inspired cognitive framework, termed the Quantum Aligned-Misaligned Entanglement Model (QAEM). This model

represents the two interacting brains within a bipartite state-space formalism, in which each subsystem is abstracted as a qubit unit ($|0\rangle$ or $|1\rangle$). Within this framework, joint configurations biased toward $|00\rangle + |11\rangle$ reflect enhanced neural alignment, whereas configurations biased toward $|01\rangle + |10\rangle$ reflect neural misalignment. The total system is described within the composite Hilbert space $C^2 \otimes C^2$, and evolves over time as an effective joint state $|\psi(t)\rangle$. Accordingly, the following Bell-type superpositions provide a convenient basis for representing interbrain connectivity within our modeling framework (49):

$$|\text{aligned}\rangle = \frac{1}{\sqrt{2}}(|00\rangle + |11\rangle), \quad |\text{misaligned}\rangle = \frac{1}{\sqrt{2}}(|01\rangle + |10\rangle).$$

In quantum information theory, it is well established that any two-qubit pure state can be written in the canonical form (86):

$$|\psi\rangle = \alpha|\mu_0\rangle + \beta \cdot e^{i\phi} \cdot |\mu_1\rangle,$$

where $|\mu_0\rangle$ and $|\mu_1\rangle$ are orthogonal states, and the entire relative phase can be absorbed into the second component. Within our quantum-inspired modeling framework, these states are cautiously interpreted as representing temporally aligned and misaligned patterns of neural activation between the two brains. At each time point t , the system's state is modeled as a linear combination of these basis states:

$$|\psi(t)\rangle = \sqrt{PLV(t)} \cdot |\text{aligned}\rangle + \sqrt{1 - PLV(t)} \cdot e^{i\phi(t)} \cdot |\text{misaligned}\rangle.$$

Here, $PLV(t)$ denotes the phase-locking value between EEG signals from two electrodes and reflects the strength of phase synchronization. $\phi(t) = WPLI(t) \cdot \pi/2$ is derived from the weighted phase lag index and is introduced to model relative phase differences between the two brains, particularly under uncoordinated parallel processing of shared task inputs.

Statistical Analysis. Behavioral and neural differences between collaborative and independent encoding were assessed using paired-sample t tests, with t -values, degrees of freedom, P -values, Cohen's d , and 95% CI reported. Pearson correlations were used to examine associations between quantum state probabilities and neural measures, including activation, PLV, and WPLI. To evaluate whether encoding-stage neural features predicted subsequent memory performance, support vector machine (SVM) classifiers were trained using entanglement states, activation, and phase-based connectivity metrics extracted from task-relevant ROIs, with performance quantified by area under the ROC curve (AUC) and significance assessed via permutation testing. Pearson correlations with permutation-based inference were additionally used to relate quantum state probabilities to individual difference measures, including trait empathy (IRI), situational empathy (SES-CC), interpersonal affinity change, and attention-switching ability (ASQ).

Data, Materials, and Software Availability. Dual-brain EEG hyperscanning data during collaborative and independent memory encoding data have been deposited in Open Science Framework, OSF (<https://osf.io/afq2pl/>) (87).

ACKNOWLEDGMENTS. This work received funding from China Postdoctoral Science Foundation 17th Batch Special Funding (2024T170591). Parts of this work were supported by the China Postdoctoral Science Foundation No.74 General Fund (2023M742431) and the Postdoctoral Fellowship Program (Grade C) of China Postdoctoral Science Foundation (GZC20231734). The present study was supported by National Natural Science Foundation of China 31671127 (C.G.)

Author affiliations: ^aBeijing Key Laboratory of Learning and Cognition, School of Psychology, Capital Normal University, Beijing 100048, China; ^bState Key Laboratory of Cognitive Science and Mental Health, Institute of Psychology, Chinese Academy of Sciences, Beijing 100101, China; ^cDepartment of Psychology, University of Chinese Academy of Sciences, Beijing 100049, China; ^dDepartment of Biomedical Engineering, School of Biological Science and Medical Engineering, Beihang University, Beijing 100191, China; ^eDepartment of Biomedical Engineering, Beijing Advanced Innovation Center for Biomedical Engineering, Beihang University, Beijing 102433, China; and ^fDepartment of Modern Physics, University of Science and Technology of China, Hefei 230026, China

Author contributions: X.Y., Y.J., Q.Z., K.P., C.G., and P.Z. designed research; X.Y., C.G., and P.Z. performed research; X.Y., Y.J., K.P., and P.Z. contributed new reagents/analytic tools; X.Y. and P.Z. analyzed data; and X.Y., C.G., and P.Z. wrote the paper.

The authors declare no competing interest.

1. S. Cheng, J. Wang, R. Luo, N. Hao, Brain to brain musical interaction: A systematic review of neural synchrony in musical activities. *Neurosci. Biobehav. Rev.* **164**, 105812 (2024).
2. A. D'Ausilio, G. Novembre, L. Fadiga, P. E. Keller, What can music tell us about social interaction? *Trends Cogn. Sci.* **19**, 111–114 (2015).
3. E. A. Solomon *et al.*, Dynamic theta networks in the human medial temporal lobe support episodic memory. *Curr. Biol.* **29**, 1100–1111.e4 (2019).
4. S. Rajaram, Collaboration both hurts and helps memory: A cognitive perspective. *Curr. Dir. Psychol. Sci.* **20**, 76–81 (2011).
5. A. P. Domanski *et al.*, Distinct hippocampal-prefrontal neural assemblies coordinate memory encoding, maintenance, and recall. *Curr. Biol.* **33**, 1220–1236.e4 (2023).
6. L. Schilbach, E. Redcay, Synchrony across brains. *Annu. Rev. Psychol.* **76**, 1–29 (2024).
7. A. F. d. C. Hamilton, Hyperscanning: Beyond the hype. *Neuron* **109**, 404–407 (2021).
8. G. Novembre, G. D. Iannetti, Hyperscanning alone cannot prove causality. Multibrain stimulation can. *Trends Cogn. Sci.* **25**, 96–99 (2021).
9. D. Paneru, E. Cohen, R. Fickler, R. W. Boyd, E. Karimi, Entanglement: Quantum or classical? *Rep. Prog. Phys.* **83**, 064001 (2020).
10. E. L. Johnson *et al.*, Dissociable oscillatory theta signatures of memory formation in the developing brain. *Curr. Biol.* **32**, 1457–1469.e4 (2022).
11. M. T. Kucewicz, J. Kamiński, Cognitive neuroscience: Theta network oscillations coordinate development of episodic memory. *Curr. Biol.* **32**, R331–R333 (2022).
12. B. Berger *et al.*, Dynamic regulation of interregional cortical communication by slow brain oscillations during working memory. *Nat. Commun.* **10**, 4242 (2019).
13. I. Gordon, A. Tomashin, O. Mayo, A theory of flexible multimodal synchrony. *Psychology. Rev.* **132**, 680–718 (2024).
14. R. Moffat, Invisible mechanisms of interpersonal alignment. *Nat. Rev. Psychol.* **3**, 146–146 (2024).
15. R. Hari, T. Himberg, L. Nummenmaa, M. Hämäläinen, L. Parkkonen, Synchrony of brains and bodies during implicit interpersonal interaction. *Trends Cogn. Sci.* **17**, 105–106 (2013).
16. C. B. Holroyd, Interbrain synchrony: On wavy ground. *Trends Neurosci.* **45**, 346–357 (2022).
17. U. Hasson, A. A. Ghazanfar, B. Galantucci, S. Garrod, C. Keysers, Brain-to-brain coupling: A mechanism for creating and sharing a social world. *Trends Cogn. Sci.* **16**, 114–121 (2012).
18. A. P. Burgess, On the interpretation of synchronization in EEG hyperscanning studies: A cautionary note. *Front. Hum. Neurosci.* **7**, 881 (2013).
19. T. Iwata *et al.*, Hippocampal sharp-wave ripples correlate with periods of naturally occurring self-generated thoughts in humans. *Nat. Commun.* **15**, 4078 (2024).
20. W. Z. Qi Zhao, C. Lu, H. Du, P. Chi, Interpersonal neural synchronization during social interactions in close relationships: A systematic review and meta-analysis of fNIRS hyperscanning studies. *Neurosci. Biobehav. Rev.* **158**, 105565 (2024).
21. J. Jiang *et al.*, Leader emergence through interpersonal neural synchronization. *Proc. Natl. Acad. Sci. U.S.A.* **112**, 4274–4279 (2015).
22. J. Wang *et al.*, Simultaneous intracranial recordings of interacting brains reveal neurocognitive dynamics of human cooperation. *Nat. Neurosci.* **28**, 161–173 (2024).
23. H. Zhang, J. Yang, J. Ni, C. K. De Dreu, Y. Ma, Leader-follower behavioural coordination and neural synchronization during intergroup conflict. *Nat. Hum. Behav.* **7**, 2169–2181 (2023).
24. M. Zhang *et al.*, Neural mechanisms distinguishing two types of cooperative problem-solving approaches: An fNIRS hyperscanning study. *Neuroimage* **291**, 120587 (2024).
25. H. Xie *et al.*, Finding the neural correlates of collaboration using a three-person fMRI hyperscanning paradigm. *Proc. Natl. Acad. Sci. U.S.A.* **117**, 23066–23072 (2020).
26. Y. Yu, "Advancements in applications of quantum entanglement" in *Journal of Physics: Conference Series*, H. B. Ahmad, O. C. Heng, R. R. Fima, Eds. (IOP Publishing, 2021), p. 012113.
27. A. Anshu, S. Arunachalam, A survey on the complexity of learning quantum states. *Nat. Rev. Phys.* **6**, 59–69 (2024).
28. E. M. Pothos, J. R. Busemeyer, Quantum cognition. *Annu. Rev. Psychol.* **73**, 749–778 (2022).
29. P. D. Bruza, Z. Wang, J. R. Busemeyer, Quantum cognition: A new theoretical approach to psychology. *Trends Cogn. Sci.* **19**, 383–393 (2015).
30. E. M. Pothos, J. R. Busemeyer, Can quantum probability provide a new direction for cognitive modeling? *Behav. Brain Sci.* **36**, 255–274 (2013).
31. A. Meghdadi, M.-R. Akbarzadeh-T, K. Javidan, A quantum-like model for predicting human decisions in the entangled social systems. *IEEE Trans. Cybern.* **52**, 5778–5788 (2022).
32. G. Gronchi, E. Strambini, Quantum cognition and Bell's inequality: A model for probabilistic judgment bias. *J. Math. Psychol.* **78**, 65–75 (2017).
33. J. R. Busemeyer, Z. Wang, R. M. Shiffrin, Bayesian model comparison favors quantum over standard decision theory account of dynamic inconsistency. *Decision* **2**, 1 (2015).
34. J. R. Busemeyer, Z. Wang, J. T. Townsend, Quantum dynamics of human decision-making. *J. Math. Psychol.* **50**, 220–241 (2006).
35. J. R. Busemeyer, Z. Wang, A. Khrennikov, I. Basieva, Applying quantum principles to psychology. *Phys. Scripta* **2014**, 014007 (2014).
36. E. Conte *et al.*, Mental states follow quantum mechanics during perception and cognition of ambiguous figures. *Open Syst. Inf. Dyn.* **16**, 85–100 (2009).
37. P. D. Kvam, T. J. Pleskac, S. Yu, J. R. Busemeyer, Interference effects of choice on confidence: Quantum characteristics of evidence accumulation. *Proc. Natl. Acad. Sci. U.S.A.* **112**, 10645–10650 (2015).
38. J.-A. Li *et al.*, Quantum reinforcement learning during human decision-making. *Nat. Hum. Behav.* **4**, 294–307 (2020).
39. J. S. Trueblood, P. Hemmer, The generalized quantum episodic memory model. *Cogn. Sci.* **41**, 2089–2125 (2017).
40. J. Denolf, A. Lambert-Mogiliansky, Bohr complementarity in memory retrieval. *J. Math. Psychol.* **73**, 28–36 (2016).
41. C. J. Brainerd, Z. Wang, V. F. Reyna, Superposition of episodic memories: Overdistribution and quantum models. *Top. Cogn. Sci.* **5**, 773–799 (2013).
42. D. L. Nelson, K. Kitto, D. Galea, C. L. McEvoy, P. D. Bruza, How activation, entanglement, and searching a semantic network contribute to event memory. *Mem. Cogn.* **41**, 797–819 (2013).
43. Á. Escobá-Gascón, Evidence of quantum-entangled higher states of consciousness. *Comput. Struct. Biotechnol. J.* **30**, 21 (2025).
44. A. Das, A. C. de Los, V. Menon, Electrophysiological foundations of the human default-mode network revealed by intracranial-EEG recordings during resting-state and cognition. *Neuroimage* **250**, 118927 (2022).
45. A. Das, V. Menon, Frequency-specific directed connectivity between the hippocampus and parietal cortex during verbal and spatial episodic memory: An intracranial EEG replication. *Cereb. Cortex* **34**, bhac287 (2024).
46. B. L. Foster, V. Rangarajan, W. R. Shirer, J. Parvizi, Intrinsic and task-dependent coupling of neuronal population activity in human parietal cortex. *Neuron* **86**, 578–590 (2015).
47. A. Das, V. Menon, Asymmetric frequency-specific feedforward and feedback information flow between hippocampus and prefrontal cortex during verbal memory encoding and recall. *J. Neurosci.* **41**, 8427–8440 (2021).
48. M. Vinck, R. Oostenveld, M. Van Wingerden, F. Battaglia, C. M. Pennartz, An improved index of phase-synchronization for electrophysiological data in the presence of volume-conduction, noise and sample-size bias. *Neuroimage* **55**, 1548–1565 (2011).
49. L. J. Fiderer, M. Kus, D. Braun, Quantum-phase synchronization. *Phys. Rev. A* **94**, 032336 (2016).
50. C. Tallon-Baudry, O. Bertrand, M.-A. Hénaff, J. Isnard, C. Fischer, Attention modulates gamma-band oscillations differently in the human lateral occipital cortex and fusiform gyrus. *Cereb. Cortex* **15**, 654–662 (2005).
51. E. A. Solomon *et al.*, Medial temporal lobe functional connectivity predicts stimulation-induced theta power. *Nat. Commun.* **9**, 4437 (2018).
52. A. Das, V. Menon, Replicable patterns of causal information flow between hippocampus and prefrontal cortex during spatial navigation and spatial-verbal memory formation. *Cereb. Cortex* **32**, 5343–5361 (2022).
53. E. A. Solomon *et al.*, Widespread theta synchrony and high-frequency desynchronization underlies enhanced cognition. *Nat. Commun.* **8**, 1704 (2017).
54. B. A. Kelsen, A. Sumich, N. Kasabov, S. H. Liang, G. Y. Wang, What has social neuroscience learned from hyperscanning studies of spoken communication? A systematic review. *Neurosci. Biobehav. Rev.* **132**, 1249–1262 (2022).
55. L. Kingsbury, W. Hong, A multi-brain framework for social interaction. *Trends Neurosci.* **43**, 651–666 (2020).
56. S. V. Wass, M. Whitehorn, I. M. Haresign, E. Phillips, V. Leong, Interpersonal neural entrainment during early social interaction. *Trends Cogn. Sci.* **24**, 329–342 (2020).
57. S. Dikker *et al.*, Brain-to-brain synchrony tracks real-world dynamic group interactions in the classroom. *Curr. Biol.* **27**, 1375–1380 (2017).
58. C. B. Holroyd, A. Umemoto, The research domain criteria framework: The case for anterior cingulate cortex. *Neurosci. Biobehav. Rev.* **71**, 418–443 (2016).
59. I. C. Fiebelkorn, S. Kastner, A rhythmic theory of attention. *Trends Cogn. Sci.* **23**, 87–101 (2019).
60. S. Aaronson, The complexity of quantum states and transformations: From quantum money to black holes. arXiv [Preprint] (2016). <https://doi.org/10.48550/arXiv.1607.05256> (Accessed 18 July 2016).
61. S. Aaronson, X. Chen, E. Hazan, S. Kale, A. Nayak, "Online learning of quantum states" in *Advances in Neural Information Processing Systems 31*, S. Bengio *et al.*, Eds. (Curran Associates, Inc, La Jolla, 2018), pp. 8962–8972.
62. S. Arunachalam, R. De Wolf, Optimal quantum sample complexity of learning algorithms. *J. Mach. Learn. Res.* **19**, 1–36 (2018).
63. R. Feldman, The neurobiology of human attachments. *Trends Cogn. Sci.* **21**, 80–99 (2017).
64. E. Redcay, L. Schilbach, Using second-person neuroscience to elucidate the mechanisms of social interaction. *Nat. Rev. Neurosci.* **20**, 495–505 (2019).
65. I. Arad, Z. Landau, U. Vazirani, T. Vidick, Rigorous RG algorithms and area laws for low energy eigenstates in 1D. *Commun. Math. Phys.* **356**, 65–105 (2017).
66. P. Ananth, L. Qian, H. Yuen, "Cryptograpy from pseudorandom quantum states" in *Annual International Cryptology Conference*, Y. Dodis, T. Shrimpton, Eds. (Springer, 2022), pp. 208–236.
67. A. L. Valencia, T. Froese, What binds us? Inter-brain neural synchronization and its implications for theories of human consciousness. *Neurosci. Conscious.* **2020**(1), nia010 (2020).
68. E. Bairey, I. Arad, N. H. Lindner, Learning a local Hamiltonian from local measurements. *Phys. Rev. Lett.* **122**, 020504 (2019).
69. C. Bădescu, R. O'Donnell, "Improved quantum data analysis" in *Proceedings of the 53rd Annual ACM SIGACT Symposium on Theory of Computing*, S. Khuller, Ed. (Association for Computing Machinery, New York, NY, 2021), pp. 1398–1411.
70. M. D. Rugg, A. P. Yonelinas, Human recognition memory: A cognitive neuroscience perspective. *Trends Cogn. Sci.* **7**, 313–319 (2003).
71. D. Aerts, S. Sozzo, T. Veloz, New fundamental evidence of non-classical structure in the combination of natural concepts. *Philos. Trans. R. Soc. Lond. A Math. Phys. Eng. Sci.* **374**, 20150095 (2016).
72. J. R. Manning, Episodic memory: Mental time travel or a quantum "memory wave" function? *Psychol. Rev.* **128**, 711 (2021).
73. S. Aaronson, Read the fine print. *Nat. Phys.* **11**, 291–293 (2015).
74. J. Zaki, Integrating empathy and interpersonal emotion regulation. *Annu. Rev. Psychol.* **71**, 517–540 (2020).
75. N. Bolger, D. Amarel, Effects of social support visibility on adjustment to stress: Experimental evidence. *J. Pers. Soc. Psychol.* **92**, 458 (2007).
76. S. Héty, V. Tschereau-Dumouchel, P. L. Jackson, Stimulating the brain to study social interactions and empathy. *Brain Stimul.* **5**, 95–102 (2012).
77. J. Decety, Dissecting the neural mechanisms mediating empathy. *Emot. Rev.* **3**, 92–108 (2011).
78. O. Jensen, J. Kaiser, J.-P. Lachaux, Human gamma-frequency oscillations associated with attention and memory. *Trends Neurosci.* **30**, 317–324 (2007).
79. X. Cui, D. M. Bryant, A. L. Reiss, NIRS-based hyperscanning reveals increased interpersonal coherence in superior frontal cortex during cooperation. *Neuroimage* **59**, 2430–2437 (2012).
80. Y. Morishima *et al.*, Task-specific signal transmission from prefrontal cortex in visual selective attention. *Nat. Neurosci.* **12**, 85–91 (2009).
81. Z. Ghanbari, M. H. Moradi, FSIFT-PLV: An emerging phase synchrony index. *Biomed. Signal Process. Control* **57**, 101764 (2020).
82. X. Li *et al.*, A novel index of functional connectivity: Phase lag based on Wilcoxon signed rank test. *Cogn. Neurodyn.* **15**, 621–636 (2021).
83. J. Chen, Y. Cui, H. Wang, E. He, A. Alhudaif, Deep learning approach for detection of unfavorable driving state based on multiple phase synchronization between multi-channel EEG signals. *Inf. Sci.* **658**, 120070 (2024).
84. P. Simor *et al.*, REM sleep microstates in the human anterior thalamus. *J. Neurosci.* **41**, 5677–5686 (2021).
85. D. Lonigro, D. Chruściński, On the classicality of quantum dephasing processes. *Front. Quant. Sci. Technol.* **1**, 1090022 (2022).
86. M. A. Nielsen, I. L. Chuang, *Quantum Computation and Quantum Information* (Cambridge University Press, Cambridge, 2001).
87. P. Zhang *et al.*, Data from "Dual-brain EEG hyperscanning data during collaborative and independent memory encoding." OSF. <https://osf.io/afq2p/>. Deposited 25 February 2026.